

# Responsive Plasmonic Assemblies of Amphiphilic Nanocrystals at Oil–Water Interfaces

Lin Cheng,<sup>†,\*</sup> Aiping Liu,<sup>†</sup> Shuo Peng,<sup>†</sup> and Hongwei Duan<sup>†,\*</sup>

<sup>†</sup>School of Chemical and Biomedical Engineering, Nanyang Technological University, 70 Nanyang Drive, Singapore 637457 and <sup>‡</sup>College of Chemistry and Materials Science, Anhui Normal University, Wuhu 241000, China

**ABSTRACT** We report a new class of amphiphilic nanocrystals with mixed polymer brush coatings, which can spontaneously assemble into two-dimensional arrays at oil–water interfaces. The plasmon coupling of gold nanoparticles and nanorods in the assembly can be reversibly modulated by conformational changes of the stimuli-responsive polymer brushes. Amphiphilic gold nanocrystals (nanoparticles and nanorods) with mixed polymer brushes were synthesized *via* sequential “grafting to” (ligand exchange) and “grafting from” (surface initiated atom transfer radical polymerization) reactions. The integration of “grafting to” and “grafting from” reactions offers great flexibility for the surface modification of the nanocrystal scaffolds, allowing the combination of polymers with distinctly different properties on well-defined nanocrystals. For nanocrystals with poly(ethylene glycol) and poly(methyl methacrylate) coatings, the collective plasmonic property of the assembly can be tailored by changing solvent quality. In the case of the amphiphilic nanocrystal with poly(ethylene glycol) and poly(2-(diethylamino)ethyl methacrylate), the pH-sensitivity of poly(2-(diethylamino)ethyl methacrylate) provides an additional means to reversibly tune the assembly by varying the pH. All of the components, including nanocrystals, materials for self-assembled monolayers (polymers and biomacromolecules) on nanocrystal surfaces, and monomers suitable for surface-initiated living radical polymerization, in this construct have a wealth of possibilities available, indicating the potential of our strategy for developing hybrid materials with integrated and collective functionalities.

**KEYWORDS:** nanocrystal · stimuli-responsiveness · self-assembly · polymer brush · surface plasmon resonance · ATRP

Metal and semiconductor nanocrystals with unique optical and electronic properties have been increasingly employed as building blocks for functional materials. Controlled assembly of nanocrystals is currently under intense research and development for a wide range of applications in electronic devices, biosensing, and drug delivery.<sup>1,2</sup> Organization of nanocrystals into superstructures often leads to collective properties that are different from those in the discrete units.<sup>1–6</sup> A prototypical example is assembled metal nanoparticles, which exhibit dramatic redshifts of surface plasmon resonance (SPR) due to strong interparticle coupling. Smart coating materials are essential to build-up metal nanoparticle-based sensing devices. For example, the use of synthetic polymers

and biomacromolecules, which are responsive to external stimuli with large conformational changes, allows for precise control over the interparticle spacing in nanoparticle superstructures and the consequent coupled spectroscopic properties,<sup>6–12</sup> leading to nanosensors for nucleic acids,<sup>6,7</sup> proteins,<sup>8</sup> metal ions,<sup>10</sup> and environmental factors such as temperature and pH.<sup>11,12</sup>

Here we report a new class of amphiphilic nanocrystals (gold nanoparticles and nanorods) with mixed polymer brush coatings, which can spontaneously assemble into two-dimensional (2-D) arrays at oil–water interfaces. Interestingly, the self-assembly is totally reversible, and the plasmon coupling of gold nanocrystals can be readily modulated by conformational changes of the stimuli-responsive polymer brushes. There are two general strategies to functionalize nanoparticles with polymer brushes. The “grafting to” method takes advantage of the reaction between nanoparticle surface and the terminal group of end-functionalized polymers; the “grafting from” method typically involves immobilization of initiators on nanoparticle surfaces and subsequent surface-initiated polymerization. Particularly, recent development in controlled radical polymerization has enabled the grafting of varieties of well-defined functional polymers on nanoparticles of diverse chemical compositions.<sup>13</sup> In this work, we have integrated the two methods and conducted sequential “grafting to” and “grafting from” reactions to prepare amphiphilic nanocrystals coated with two mixed polymer brushes with distinctly different chemical composition and properties. Grafting a layer of polymer brushes on nanocrystals has led to hybrid nanoparticles with enhanced colloidal stability, stimuli-responsiveness, and improved

\*Address correspondence to hduan@ntu.edu.sg.

Received for review July 19, 2010 and accepted September 2, 2010.

Published online September 10, 2010. 10.1021/nn101685q

© 2010 American Chemical Society

biocompatibility.<sup>13–15</sup> Nanocrystals with mixed polymer brushes are typically prepared by the “grafting to” method.<sup>16–20</sup> Amphiphilic nanocrystals with polymer brush coatings have shown unique self-assembly properties in selective solvents of their individual components, forming nanostructures with tunable morphologies and collective properties.<sup>9,20,21</sup> On the other hand, accumulating evidence has shown that nanoparticles with rationally designed surfaces have the tendency to assemble at liquid–liquid interfaces due to the decrease in total free energy.<sup>22,23</sup> Thus, oil–water interfaces have emerged as a flexible platform to prepare large areas of close-packed nanocrystal arrays.<sup>9,10</sup> However, it remains a challenge to obtain interfacial assemblies of nanocrystals with reversible and readily tailored collective properties.<sup>24</sup> Here, we have shown that our synthetic approach gives rise to robust nanoparticles with excellent colloidal stability in various aqueous and organic solvents, and more importantly, interfacial assemblies of the amphiphilic nanocrystals with mixed polymer brush coatings exhibit a collection of unique features including stimuli-triggered assembly–disassembly with fast kinetics and flexibly controlled nanocrystal spacing in their arrays.

## RESULTS AND DISCUSSION

Amphiphilic gold nanocrystals with environmentally responsive mixed polymer brushes were synthesized *via* combined “grafting to” and “grafting from” strategies. As illustrated in Figure 1, citrate-stabilized 14 nm gold nanoparticles were capped with a binary mixture of methoxy-poly(ethylene glycol)-thiol (PEG, MW = 5 kDa) and 2,2′-dithiobis[1-(2-bromo-2-methylpropionyloxy)]ethane (DTBE), an initiator of atom-transfer radical polymerization (ATRP), by a ligand-exchange reaction. The molar ratio of PEG and DTBE is 1:5, and the overall thiol added is 2 orders of magnitude higher than that needed to saturate the nanoparticle surfaces (see Supporting Information) to ensure a complete ligand exchange. The nanocrystal was purified by centrifugation and ultrafiltration of its ethanol solution. <sup>1</sup>H NMR spectra (see Supporting Information) of the nanocrystal coated with PEG and DTBE (Au@PEG/DTBE) show the resonance of PEG at 3.65 ppm and two broad resonances at 1.2–1.4 and 0.8–0.9 ppm,<sup>25,26</sup> which are typical resonances of methylene and methyl groups of alkanethiol ligands on gold nanoparticle surfaces, suggesting that free, unbounded PEG and DTBE are completely removed. Coadsorption of PEG and the initiator led to robust nanocrystals that form stable dispersions in a number of solvents such as water, chloroform, and dimethylformamide (DMF). Recent advances in ATRP have enabled the polymerization of a wide range of vinyl-based monomers in a controlled manner.<sup>27</sup> The general solubility of Au@PEG/DTBE coupled with surface-initiated ATRP have provided opportunities to synthesize varieties of am-

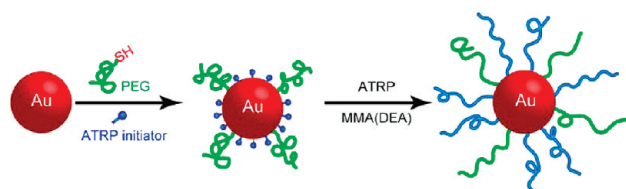


**Figure 1.** Schematic illustration of the synthesis of amphiphilic gold nanocrystals in the sequentially combined “grafting to” (coadsorption PEG and ATRP initiator) and “grafting from” (surface-initiated ATRP) approaches.

phiphilic nanocrystals with well-defined mixed polymer brush coatings. Here, poly(methyl methacrylate) (PMMA) or poly(2-(diethylamino)ethyl methacrylate) (PDEA) were grafted from Au@PEG/DTBE in DMF at 40 °C using CuBr/*N,N,N',N',N''*-pentamethyldiethylenetriamine (PMDETA) as the ATRP catalyst.<sup>28</sup> The mild polymerization condition is chosen to avoid any possible detachment of ligands from gold nanocrystal surfaces. Nanocrystals with mixed polymer brush coatings were separated by centrifugation after polymerization, and no polymer was detected in the supernatant.

Amphiphilic gold nanoparticles with PEG and PMMA brushes (Au@PEG/PMMA) are dispersible in both water and organic solvents such as chloroform and DMF. It is expected that both PEG and PMMA grafts are stretched and exist in brush conformation in their common solvents, *i.e.*, chloroform, whereas in selective solvents of

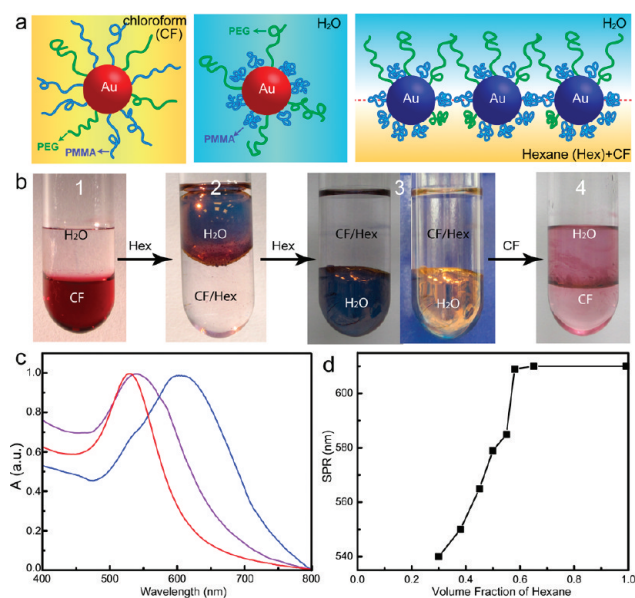


**Figure 2.** Interfacial assembly of gold nanocrystals with mixed PEG and PMMA brushes. (a) Schemes of the nanocrystal in chloroform and water and at interfaces. (b) Photographs of the assembling process: image 1 shows the mixture of 1.5 mL of H<sub>2</sub>O and 1.5 mL of gold nanocrystals chloroform solution; image 2 shows the assembly upon addition of hexane (40% volume fraction of the organic phase); image 3 shows the assembly when hexane volume fraction is 80%; and image 4 captures the moment of replacing the hexane–chloroform mixture with pure chloroform, which shows the dissolution of the assembly upon addition of chloroform. (c) UV–vis spectra of the nanocrystal in chloroform (red line), at the interface of water and hexane–chloroform mixtures (purple line, 30% hexane; blue line, 80% hexane). (d) Dependence of SPR peaks on the volume fraction of hexane in the oil phase.

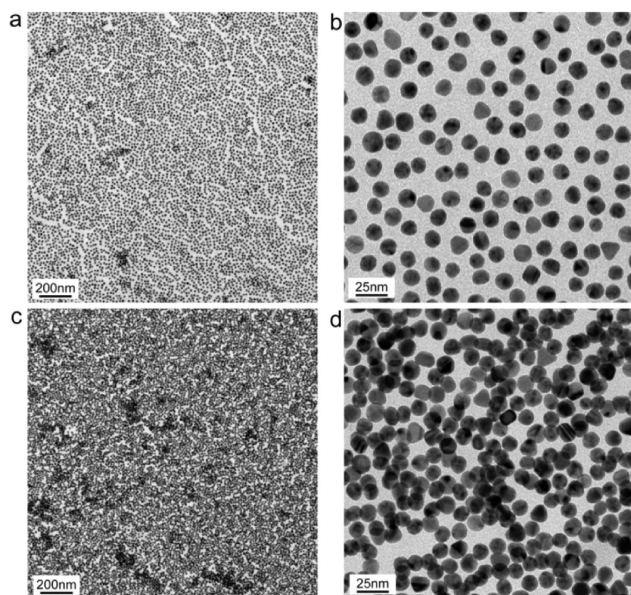


**Figure 3.** TEM images of the gold nanoparticle assembly with 540 nm SPR peak (a,b) and the assembly with 612 nm SPR peak (c,d) at different magnifications.

PEG such as water, PMMA collapse and are shielded by the soluble PEG grafts (Figure 2a).  $^1\text{H}$  NMR analysis of the nanoparticle and gel permeation chromatography of the PMMA ( $M_{n(\text{PMMA})} = 22$  kDa, PDI = 1.26) cleaved from the nanoparticle surface suggest that PEG and PMMA have a molar ratio of 1:2 in Au@PEG/PMMA (see Supporting Information). Combining this ratio with a 20% organic fraction determined by thermogravimetric analysis (TGA) leads to a graft density of 0.43 chain/ $\text{nm}^2$ , which corresponds to 264 polymer grafts (88 PEG chains and 176 PMMA chains) per nanoparticles (see Supporting Information). This graft density is comparable to the density obtained by surface-initiated polymerization on Au nanoparticles in previous reports.<sup>29</sup> In a mixture of water and chloroform, the amphiphilic nanoparticles prefer to stay in chloroform due to favorable solubility of PMMA (Figure 2b). Assembly of Au@PEG/PMMA can be triggered by adding hexane, which is a nonsolvent of both PEG and PMMA, into this biphasic system, leading to a separated layer between the two phases. This layer (Figure 2b) shows characteristic golden-color reflectance and purple/blue transmittance due to the strong coupling of gold nanocrystals in close proximity.<sup>23</sup> When the volume fraction of hexane reaches 30% of the organic phase, nearly 100% of the nanoparticles in chloroform move to the interface within 1–2 min under gentle shaking. Cuvettes with silylated surfaces allow the measurement of UV–vis spectra (Figure 2c) of the assembly *in situ*, which shows that the SPR band (540 nm) of the assembly red-shifted relative to that (528 nm) of the isolated nanoparticle in dispersion. Interestingly, the SPR peak (Figure 2d) showed continuous red-shifting to 612 nm until the volume fraction of hexane in the oil phase reached 0.60. The significant red-shift of the SPR band upon increas-

ing hexane in the oil phase should be a result of the continuous collapse of the mixed brushes, which reduces the separating distance of neighboring nanoparticles and also increases the local refractive indexes. Both of those factors could cause the red-shift of SPR.<sup>30</sup> Transmission electron microscopy (TEM) images (Figure 3) of the nanocrystal film dip-coated on a carbon-coated copper grid show that gold nanoparticles form 2-D arrays without long-range order (the polymer part is not visible because of its poor contrast). Evidently, nanoparticles in the assembly with 540 nm SPR peak exhibit larger interparticle distance than those in the assembly with 612 nm SPR peak. Our strategy represents a facile approach to reversibly controlling the average spacing of nanocrystals in their 2-D arrays, offering great advantages over the assemblies of nanocrystals with small molecular capping ligands.<sup>22,23</sup> Previously, the control of nanoparticle spacing can only be realized in the array of DNA-functionalized nanoparticles<sup>31</sup> or hydrophobic nanoparticles formed at the water/air interface by using the Langmuir–Blodgett technique.<sup>29</sup> The assembly obtained here can potentially serve as a new type of nanosensors (*i.e.*, for reactions at interfaces) and templating substrate.<sup>1,2</sup>

The amphiphilic nature of the gold nanoparticle plays important roles in forming stable interfacial assemblies. Without the aqueous phase, Au@PEG/PMMA forms aggregates and eventually precipitates from the solution when increasing amounts of hexane are added. The precipitation is obviously due to the collapse of PMMA and PEG brushes when the environment changes from a good solvent to a nonsolvent. However, in the biphasic system, the affinity of PEG for aqueous phase can stabilize the assembly and prevent aggregation from happening (Figure 2a). Remarkably, we find that replacing the hexane–chloroform mixture with pure chloroform leads to immediate dissolution of nanocrystals into the oil phase (Figure 2b), indicating the dynamic nature of the assembly. This assembly–dissolution process can be repeated many times without affecting the colloidal stability of the nanocrystals. Similarly, adding DMF pulls the nanocrystals from water–hexane interfaces into the aqueous phase. The phase transfer of amphiphilic nanocrystals with interfacial accumulation as an intermediate stage could provide new insights to design functional materials for phase-selective applications.

Surface functionalization with sequential “grafting to” and “grafting from” of polymer brushes offers great flexibility to integrate stimuli-responsive polymers on nanocrystal scaffolds. Weak polyelectrolyte brushes, responding to pH variation with large conformational and solubility changes, have found uses in many applications, such as surface coating and controlled drug delivery.<sup>32</sup> PDEA has a  $\text{pK}_a$  of 7.3, experiencing a hydrophilic-to-hydrophobic transition when the solution pH rises above its  $\text{pK}_a$ .<sup>33</sup> Gold nanoparticles with PEG and PDEA

grafts (Au@PEG/PDEA) are dispersed very well in aqueous solutions and in organic solvents, which are good solvents (chloroform and DMF) for both brushes. However, in a biphasic system of aqueous solution and chloroform, Au@PEG/PDEA stays in different phases, depending on the pH of the aqueous solution. For example, in the mixture of pH 3.0 water and chloroform, the nanocrystal is in the aqueous phase; the nanocrystal shows a preference for the organic phase when pH 10.0 water is used. This is obviously due to protonation and deprotonation of the pendant tertiary amine groups of PDEA at different pH. Protonated PDEA at pH 3.0 is only soluble in water; at pH 10.0, deprotonated PDEA is hydrophobic and can only be dissolved in chloroform. As a result, alternating pH of the aqueous phase leads to reversible phase transfer of Au@PEG/PDEA between the aqueous and organic phases. Upon the change of pH, 90% of the particle is quickly transferred to the other phase within 1 min under gentle shaking.

The pH-sensitivity of PDEA provides an additional means to regulate the interfacial assembly besides the change of solvent quality used for the controlled assembly of Au@PEG/PMMA. As shown in Figure 4, the interfacial assembly of Au@PEG/PDEA, exhibiting golden-color reflectance and purple transmittance, can be stimulated by NaOH titration in the biphasic system of acidic water and chloroform–hexane mixture. Again, the amphiphilic nanocrystal can also be pulled back to the aqueous phase by adding HCl, and this self-assembly can be reversibly switched by alternating pH. Our results have shown that self-assembly of the gold nanoparticles at the oil–water interface (Figure 4b), induced by the hydrophilic-to-hydrophobic transition of the PDEA grafts, results in assemblies with a broader and red-shifted SPR peak. Similarly, adding hexane in the mixture of basic water and chloroform also leads to the assembly due to the change of solvent quality for PDEA in the organic phase. The combination of these two approaches (pH variation and change of solvent quality) gives rise to new possibilities to modulate the plasmonic properties of the nanocrystal ensembles.

Anisotropic gold nanorods have two distinct SPR bands: a strong, long-wavelength band arising from the longitudinal oscillation of the conduction band electrons and a weak, short-wavelength band due to the transverse electron oscillation. Recent research has demonstrated the potential applications of gold nanorods for bioimaging, photothermal therapy, and surface-enhanced Raman scattering.<sup>34</sup> Here, gold nanorods covered with a double layer of cetyl trimethylammonium bromide (CTAB) were synthesized *via* a seeded growth approach.<sup>35</sup> The obtained gold nanorods have an aspect ratio of 3.1 (13 nm in width), and the longitudinal SPR band is centered at 706 nm. “Grafting to” of end-functionalized polymers on gold nanorods have been reported by several groups.<sup>9,36–38</sup> Here, a two-step ligand exchange was used for the “grafting to” re-

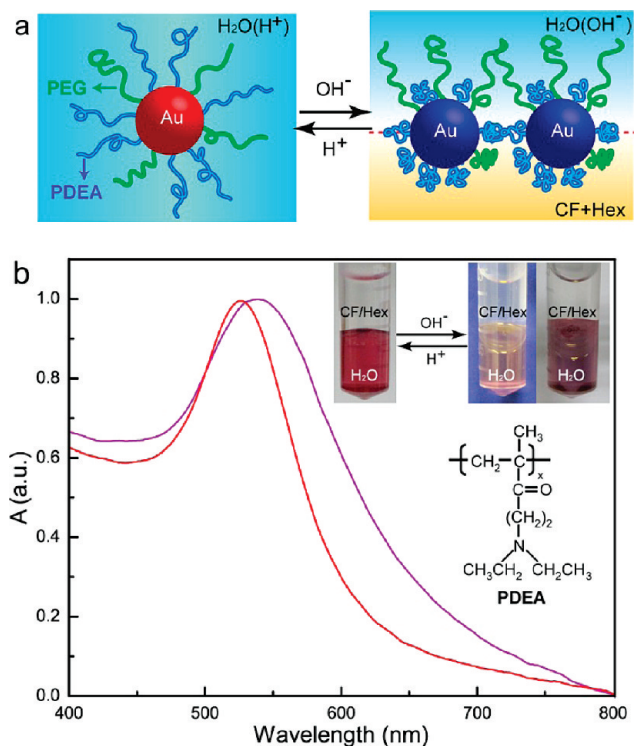


**Figure 4.** (a) Schematic diagrams of the assembly of Au@PEG/PDEA controlled by pH variation. (b) UV–vis spectra of nanocrystals dissolved in pH 3 water (red line) and the assembly at interfaces of chloroform and hexane (volume fraction of hexane is 80%) and pH 10 water (purple line). Inset: Photographs of the nanocrystal and the assembly, and chemical structure of PDEA.

action between CTAB-coated gold nanoparticles and the PEG/DTBE ligands. In the first step, gold nanorods aggregated 2 h after addition of a DMF solution of PEG and DTBE. The aggregated nanorods can be redissolv-

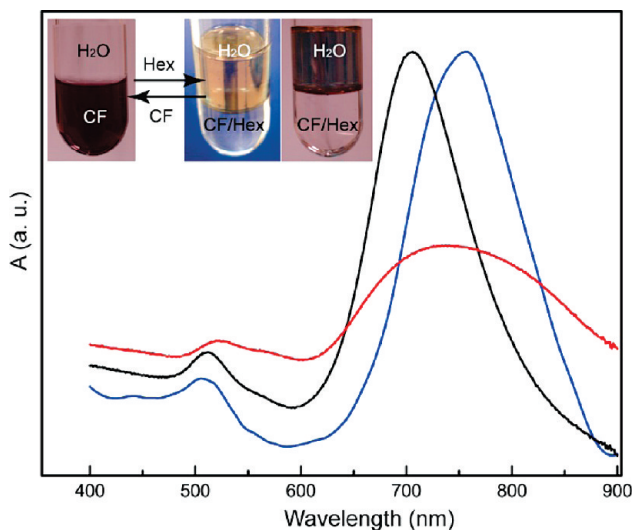


**Figure 5.** UV–vis spectra of gold nanorods and their assemblies: CTAB-covered gold nanorods (black line), amphiphilic nanorods coated with mixed polymer brushes of PEG and PMMA (blue line), and interfacial assembly of the amphiphilic nanorods (red line). Inset: Photographs showing the reversible self-assembly of the amphiphilic nanorods (volume fraction of hexane in the organic phase is 30%).

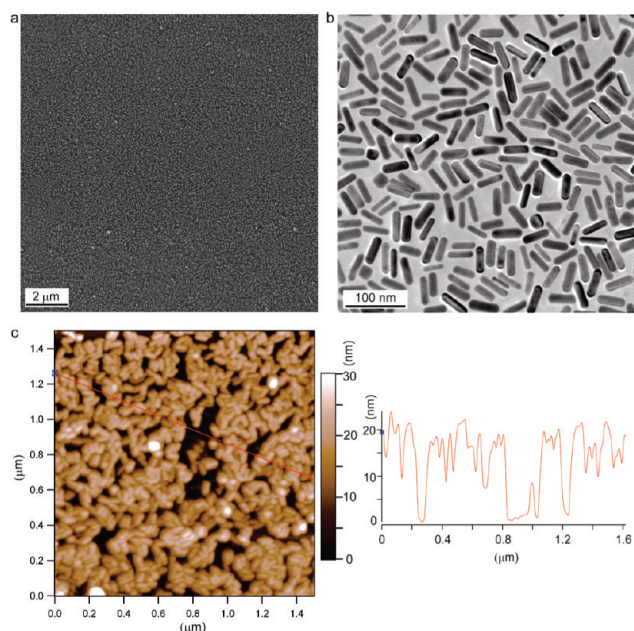


**Figure 6.** Morphological characterization of the interfacial assembly of the amphiphilic gold nanorods transferred on substrates. (a) SEM image, (b) TEM image, (c) AFM image and the corresponding height profile.

led in DMF and form a very stable dispersion. The loss of water-solubility indicates the partial removal of CTAB coating. In the second step of ligand exchange, additional PEG/DTBE ligands were introduced, and the nanorods were recovered by centrifugation after 24 h of reaction.  $^1\text{H}$  NMR spectra have shown that the characteristic peaks of CTAB in the original nanorods are not detected in the nanorods after surface modification, indicating the CTAB coating is nearly completely removed (see Supporting Information). PMMA brushes were grafted from the nanorods in a surface-initiated ATRP reaction similar to that used for spherical nanoparticles. Due to the introduction of PMMA brushes, the coated nanorods became soluble in chloroform, which is a nonsolvent for original nanorods. As shown in Figure 5, the longitudinal SPR of gold nanorods showed a red-shift of 50 nm to 756 nm in PEG-PMMA mixed polymer brush coated nanorods (AuNR@PEG/PMMA). In comparison, a shift of only 8 nm was observed for spherical nanoparticles. This is in agreement with the notion that the longitudinal SPR band of gold nanorods is highly sensitive to the variation of local environment, exhibiting a greater wavelength red-shift in response to the increase of refractive index than that of

spherical gold nanoparticles.<sup>39</sup> Similar to the Au@PEG/PMMA nanoparticles, interfacial assembly of the AuNR@PEG/PMMA nanorods can be induced by adding hexane into the biphasic system of water and chloroform solution of the amphiphilic nanorods (inset in Figure 5). *In situ* UV-vis spectroscopic measurement shows that interparticle coupling leads to a much broader longitudinal band and a red-shifted transverse absorption relative to those of the nanorods in solution; the slight blue-shift of the longitudinal peak could be due to the tendency of the nanorods to form parallel packing in the assembly, as shown in Figure 6. Figure 6a is a representative scanning electron microscopy (SEM) image of the assembly transferred on silicon substrate, revealing large-area homogeneous 2-D arrays of gold nanorods. Both TEM and SEM images show that the nanorods lie horizontally at the oil-water interfaces. The height of the assembly measured by atomic force microscopy (AFM) is about 21 nm, which is 8 nm bigger than the diameter of the gold nanorods. This obviously is due to the presence of the polymer brushes on the nanorods surface, although the polymer coating is not visible in the TEM image. Our results on the gold nanoparticles and nanorods with the same polymer brush coatings demonstrate that the interfacial self-assembly of nanocrystals is primarily modulated by their surface properties and have no significant correlation with their shapes.

## CONCLUSIONS

In summary, we have developed a new approach to exploit amphiphilic nanocrystals with responsive mixed polymer brush coatings toward interfacial assemblies with reversible and tunable plasmonic properties. The strategy with integrated and sequential “grafting to” and “grafting from” reactions offers great flexibility for the surface modification of the nanocrystal scaffolds, allowing the combination of polymers with distinctly different properties on well-defined nanocrystals. All of the components, including nanocrystals,<sup>1–5</sup> materials for self-assembled monolayer (polymers and biomacromolecules) on nanocrystal surfaces,<sup>1,2</sup> and monomers suitable for surface-initiated living radical polymerization,<sup>27,40</sup> in this construct have a wealth of possibilities available, indicating the potential of our strategy for developing hybrid materials with integrated and collective functionalities.

## EXPERIMENTAL SECTION

Materials are obtained from Sigma-Aldrich unless specified otherwise. Methoxy-poly(ethylene glycol)-thiol (PEG) with a molecular weight of 5000 Da was purchased from Laysan Bio, Inc. Chloroauric acid was obtained from Alfa Aesar. Transmission electron microscopy observations were conducted on a Jeol JEM 2010 electron microscope at an acceleration voltage of 200 kV. Scanning electron microscopy image were obtained on a FESEM

instrument (JSM-6700F, Japan). Atomic force microscopy measurements were conducted on a MFP-3D microscope (Asylum research). A KSV DC dip-coater was used to transfer the assembly on substrates. UV-vis absorption spectra were recorded by using a Thermo Electron UV-vis spectrophotometer (NICOLET evolution 500).  $^1\text{H}$  NMR characterization was conducted at Bruker AV300, using  $\text{CDCl}_3$  or  $\text{D}_2\text{O}$  as the solvent. Gel permeation chromatography was measured on a Shimadzu HPLC system using

THF as the eluent, and the molecular weight was calibrated with polystyrene standards. Polymer grafts were cleaved from the nanoparticles by treating the nanoparticles with 5 mM iodine solution in dichloromethane, and PMMA was separated from PEG by precipitating the solution in methanol. Thermogravimetric analysis was performed on a Perkin-Elmer Diamond TG/DTA. Samples were placed in platinum sample pans and heated under a nitrogen atmosphere at a rate of 10 °C/min to 100 °C and held for 30 min to completely remove residual solvent. Samples were then heated to 700 °C at a rate of 10 °C/min.

**Synthesis of Gold Nanoparticles.** Uniform 14-nm-diameter gold nanoparticles were prepared by citrate reduction of HAuCl<sub>4</sub> in aqueous phase. Typically, a sodium citrate (205 mg) deionized water solution (4 mL) was rapidly injected into a boiling aqueous HAuCl<sub>4</sub> (61 mg in 400 mL of water) solution under vigorous stirring. After boiling for 15 min, the solution was cooled to room temperature. TEM analysis of more than 200 particles gave a standard deviation in diameter of the obtained gold nanoparticles of <10%.

**Gold Nanorods Synthesis.** Original CTAB-stabilized Au nanorods (AuNR@CTAB) were synthesized by a seeded growth method at 30 °C through reduction of HAuCl<sub>4</sub> with ascorbic acid in the presence of CTAB and AgNO<sub>3</sub> according to the method reported previously.<sup>35</sup> After being purified by centrifugation (8000g, 30 min) three times, AuNR@CTAB was stored in water for further use. The nanorods have an average aspect ratio of 3.1 and a diameter of 13 nm.

**"Grafting to" Reaction on Gold Nanoparticles.** Au@PEG/DTBE was prepared by coadsorption of PEG and DTBE ligand through the Au-S bond. In brief, a solution of PEG (50 mg) and DTBE (23 mg) in DMF (2 mL) was slowly added into 100 mL of the original 14 nm Au nanoparticles (3.3 nM) in water. After the solution was stirred overnight, nanocrystals were recovered by centrifugation (8000g, 25 min). Any free polymers and DTBE present were removed by ultrafiltration (cutoff = 100 kDa) of an ethanol solution of the nanocrystals. Au@PEG/DTBE can be stored in chloroform or DMF for further use.

**"Grafting to" Reaction on Gold Nanorods.** Typically, a solution (solution A) of PEG (30 mg) and DTBE (10 mg) in DMF (2 mL) was added slowly into 2 mL (21 nM) of the original AuNR@CTAB in water. Notably, there are two steps for this ligand-exchange reaction. In the first step, nanorods aggregated 2 h after addition of 0.5 mL of solution A. The nanorods were collected by centrifugation and redispersed in DMF. In the second step, the remaining solution A (~1.5 mL) was mixed with the DMF solution of the nanorods. After being stirred for 24 h, the reaction mixture was still a clear solution, and the coated nanorods were purified by repeated centrifugation (8000g, 30 min) and redispersion more than 3 times.

**"Grafting from" Reactions.** Surface-initiated ATRP was used for the synthesis of amphiphilic nanocrystals of Au@PEG/PMMA and Au@PEG/PDEA. Typically, 0.2 mL of monomer (MMA or DEA) and the initiator-coated gold nanocrystals (0.1 nmol) were mixed in DMF (2.0 mL). After the mixture was deaerated for 30 min by nitrogen, CuBr (4 mg) and PMDETA (15 mg) were introduced to initiate the polymerization. The reaction was carried out at 40 °C for 10 h. Catalysts and unreacted monomer were removed by repeated centrifugation, and the amphiphilic nanocrystals were stored as water or chloroform solutions as needed.

**Self-Assembly of Amphiphilic Nanocrystals at Oil-Water Interfaces.** Equal volumes of deionized water and chloroform solution of amphiphilic nanocrystals with PEG and PMMA coatings were mixed in a glass tube with silanated surfaces or a plastic centrifuge vial. To induce the self-assembly of the nanocrystal, hexane was added slowly and mixed well by gentle shaking. The *in situ* UV-vis spectra of the film were measured using a quartz cuvette with silanated surfaces. Assembly of Au@PEG/PDEA nanoparticles at the interface of water and the mixture of chloroform and hexane was induced by adding pH 13.0 NaOH solution in the aqueous phase, and alternating pH was realized by adding pH 1.0 HCl.

**Acknowledgment.** H.D. thanks the program of Nanyang Assistant Professorship for financial support. This work is also partially supported by National Nature Science Foundation of China

(20904001) and NSF of Anhui Province (090414198) to L.C. We are grateful to Jinhua Hu for helpful discussion and Jindui Hong for assistance in TGA measurements.

**Supporting Information Available:** Additional experimental details and supporting spectroscopy and imaging data. This material is available free of charge via the Internet at <http://pubs.acs.org>.

## REFERENCES AND NOTES

- Min, Y.; Akbulut, M.; Kristiansen, K.; Golan, Y.; Israelachvili, J. The Role of Interparticle and External Forces in Nanoparticle Assembly. *Nat. Mater.* **2007**, *7*, 527–538.
- Nie, Z. H.; Petukhova, A.; Kumacheva, E. Properties and Emerging Application of Self-Assembled Structures Made from Inorganic Nanoparticles. *Nat. Nanotechnol.* **2010**, *5*, 15–25.
- Ghosh, S. K.; Pal, T. Interparticle Coupling Effect on the Surface Plasmon Resonance of Gold Nanoparticles: From Theory to Applications. *Chem. Rev.* **2007**, *107*, 4797–4862.
- Claridge, S. A.; Castlman, S. N.; Khanna, S. N.; Murray, C. B.; Sen, A.; Weiss, P. S. Cluster-Assembled Materials. *ACS Nano* **2009**, *3*, 244–255.
- Srivastava, S.; Kotov, N. A. Nanoparticle Assembly for 1D and 2D Ordered Structures. *Soft Matters* **2007**, *3*, 1146–1156.
- Rosi, N. L.; Mirkin, C. A. Nanostructures in Biodiagnostics. *Chem. Rev.* **2005**, *105*, 1547–1562.
- Elghanian, R.; Storhoff, J. J.; Mucic, R. C.; Letsinger, R. L.; Mirkin, C. A. Selective Colorimetric Detection of Polynucleotides Based on the Distance-Dependent Optical Properties of Gold Nanoparticles. *Science* **1997**, *277*, 1078–1081.
- Wang, Z. X.; Levy, R.; Fernig, D. G.; Brust, M. Kinase-Catalyzed Modification of Gold Nanoparticles: A New Approach to Colorimetric Kinase Activity Screening. *J. Am. Chem. Soc.* **2006**, *128*, 2214–2215.
- Nie, Z. H.; Fava, D.; Kumacheva, E.; Zou, S.; Walker, G. C.; Rubinstein, M. Self-Assembly of Metal-Polymer Analogues of Amphiphilic Triblock Copolymers. *Nat. Mater.* **2007**, *6*, 609–614.
- Kim, S.; Park, J. W.; Kim, D.; Kim, D.; Lee, I. H.; Jon, S. Bioinspired Colorimetric Detection of Calcium Ions in Serum Using Calsequestrin-Functionalized Gold nanoparticles. *Angew. Chem., Int. Ed.* **2009**, *48*, 4138–4141.
- Zhu, M. Q.; Wang, L. Q.; Exarhos, G. J.; Li, A. D. Q. Thermosensitive Gold Nanoparticles. *J. Am. Chem. Soc.* **2004**, *126*, 2656–2657.
- Shen, Y.; Kuang, M.; Shen, Z.; Nieberle, J.; Duan, H. W.; Frey, H. Gold Nanoparticles Coated with a Thermosensitive Hyperbranched Polyelectrolyte: Towards Smart Temperature and pH Nanosensors. *Angew. Chem., Int. Ed.* **2008**, *47*, 2227–2230.
- Barbey, R.; Lavanant, L.; Paripovic, D.; Schüwer, N.; Sugnaux, C.; Tugulu, S.; Klok, H. A. Polymer Brushes via Surface-Initiated Controlled Radical Polymerization: Synthesis, Characterization, Properties, and Applications. *Chem. Rev.* **2009**, *109*, 5437–5527.
- Zhao, B.; Zhu, L. Mixed Polymer Brush-Grafted Particles: A New Class of Environmentally Responsive Nanostructured Materials. *Macromolecules* **2009**, *42*, 9369–9383.
- Jia, H.; Titmuss, S. Polymer-Functionalized Nanoparticles: from Stealth Viruses to Biocompatible Quantum Dots. *Nanomedicine* **2009**, *4*, 951–966.
- Shan, J.; Nuopponen, M.; Jiang, H.; Viitala, T.; Kauppinen, E.; Kontturi, K.; Tenhu, H. Amphiphilic Gold Nanoparticles Grafted with Poly(N-isopropylacrylamide) and Polystyrene. *Macromolecules* **2005**, *38*, 2918–2926.
- Shan, J.; Chen, J.; Nuopponen, M.; Viitala, T.; Jiang, H.; Peltonen, J.; Kauppinen, E.; Tenhu, H. Optical Properties of Thermally Responsive Amphiphilic Gold Nanoparticles Protected with Polymers. *Langmuir* **2006**, *22*, 794–801.
- Genson, K. L.; Holzmüller, J.; Jiang, C.; Xu, J.; Gibson, J. D.; Zubarev, E. R.; Tsukruk, V. V. Langmuir-Blodgett Monolayer of Gold Nanoparticles with Amphiphilic Shells from V-

- Shaped Binary Polymer Arms. *Langmuir* **2006**, *22*, 7001–7015.
19. Zubarev, E. R.; Xu, J.; Sayyad, A.; Gibson, J. D. Amphiphilic Gold Nanoparticles with V-Shaped Arms. *J. Am. Chem. Soc.* **2006**, *128*, 4958–4959.
  20. Zubarev, E. R.; Xu, J.; Sayyad, A.; Gibson, J. D. Amphiphilicity-Driven Organization of Nanoparticles into Discrete Assemblies. *J. Am. Chem. Soc.* **2006**, *128*, 15098–15099.
  21. Nikolic, M. S.; Olsson, C.; Salcher, A.; Kornowski, A.; Rank, A.; Schubert, R.; Frömsdorf, A.; Weller, H.; Förster, S. Micelle and Vesicle Formation of Amphiphilic Nanoparticles. *Angew. Chem., Int. Ed.* **2009**, *48*, 2752–2754.
  22. Lin, Y.; Skaff, H.; Emrick, T.; Dinsmore, A. D.; Russell, T. P. Nanoparticle Assembly and Transport at Liquid-Liquid Interfaces. *Science* **2003**, *299*, 226–229.
  23. Duan, H. W.; Wang, D. Y.; Kurth, D. G.; Möhwald, H. Directing Self-Assembly of Nanoparticles at Water/Oil Interfaces. *Angew. Chem., Int. Ed.* **2004**, *43*, 5639–5642.
  24. Böker, A.; He, J.; Emrick, T.; Russell, T. P. Self-Assembly of Nanoparticles at Interfaces. *Soft Matter* **2007**, *3*, 1231–1248.
  25. Shon, S.; Gross, S.; Dawson, M. B.; Porter, M.; Murray, R. W. Alkanethiolate-Protected Gold Clusters from Sodium S-Dedecylthiosulfate (Bunte Saltes). *Langmuir* **2000**, *16*, 6555–6561.
  26. Zhang, S. S.; Leem, G.; Lee, T. T. Monolayer-Protected Gold Nanoparticles Prepared Using Long-Chain Alkanthioacetates. *Langmuir* **2009**, *25*, 13855–13860.
  27. Matyjaszewski, K.; Xia, J. Atom Radical Transfer Polymerization. *Chem. Rev.* **2001**, *101*, 2921–2990.
  28. Duan, H. W.; Kuang, M.; Wang, D. Y.; Kurth, D. G.; Möhwald, H. Colloidally Stable Amphibious Nanocrystals Derived from Poly[2-(dimethylamino)ethyl methacrylate] Capping. *Angew. Chem., Int. Ed.* **2005**, *44*, 1717–1720.
  29. Ohno, K.; Koh, K.; Tsujii, Y.; Fukuda, T. Fabrication of Ordered Arrays of Gold Nanoparticles Coated with High-Density Polymer Brushes. *Angew. Chem., Int. Ed.* **2003**, *42*, 2751–2754.
  30. Ung, T.; Liz-Marzán, L. M.; Mulvaney, P. Optical Properties of Thin Films of Au@SiO<sub>2</sub> Particles. *J. Phys. Chem. B* **2001**, *105*, 3441–3452.
  31. Cheng, W.; Campolongo, M. J.; Cha, J. J.; Tan, S. J.; Umbach, C. C.; Muller, D. A.; Luo, D. Free Standing Nanoparticle Superlattice Sheets Controlled by DNA. *Nat. Mater.* **2009**, *8*, 519–525.
  32. Stuart, M. A. C.; Huck, W. T. S.; Genzer, J.; Müller, M.; Ober, C.; Stamm, M.; Sukhorukov, G. B.; Szleifer, I.; Tsukruk, V. T.; Urban, M.; et al. Emerging Applications of Stimuli-Responsive Polymer Materials. *Nat. Mater.* **2010**, *9*, 101–113.
  33. Bütün, V.; Armes, S. P.; Billingham, N. C. Synthesis and Aqueous Solution Properties of Near-Monodisperse Tertiary Amine Methacrylate Homopolymers and Diblock Copolymers. *Polymer* **2001**, *42*, 5993–6008.
  34. Jain, P. K.; Huang, X. H.; El-Sayed, I. H.; El-Sayed, M. A. Noble Metals on the Nanoscale: Optical and Photothermal Properties and Some Applications in Imaging, Sensing, Biology, and Medicine. *Acc. Chem. Res.* **2008**, *41*, 1578–1586.
  35. Nikoobakht, B.; El-Sayed, M. A. Preparation and Growth Mechanism of Gold Nanorods (NRs) Using Seed-Mediated Growth Method. *Chem. Mater.* **2003**, *15*, 1957.
  36. Liao, H. W.; Hafner, J. H. Gold Nanorod Bioconjugates. *Chem. Mater.* **2005**, *17*, 4636–4641.
  37. Khanal, B. P.; Zubarev, E. R. Rings of Nanorods. *Angew. Chem., Int. Ed.* **2007**, *46*, 2195–2198.
  38. Khanal, B. P.; Zubarev, E. R. Polymer-Functionalized Platinum-On-Gold Bimetallic Nanorods. *Angew. Chem., Int. Ed.* **2009**, *48*, 6888–6891.
  39. Nie, Z. H.; Fava, D.; Kumacheva, E.; Ruda, H. E.; Shik, A. Plasmon Spectra in Two-Dimensional Nanorod Arrays. *Nanotechnology* **2009**, *20*, 295203.
  40. Moad, G.; Rizzardo, E.; Thang, S. H. Towards Living Radical Polymerization. *Acc. Chem. Res.* **2008**, *41*, 1133–1142.